The chiral critical point of $N_f = 3$ QCD at finite density to the order $(\mu/T)^4$

Philippe de Forcrand[1,2] and Owe Philipsen[3]

[1] *Institut für Theoretische Physik, ETH Zürich, CH-8093 Zürich, Switzerland*
[2] *CERN, Physics Department, TH Unit, CH-1211 Geneva 23, Switzerland*
[3] *Institut für Theoretische Physik, Westfälische Wilhelms-Universität Münster,
Germany*

Abstract

QCD with three degenerate quark flavours at zero baryon density exhibits a first order thermal phase transition for small quark masses, which changes to a smooth crossover for some critical quark mass m_0^c, i.e. the *chiral* critical point. It is generally believed that as an (even) function of quark chemical potential, the critical point $m_c(\mu)$ moves to larger quark masses, constituting the critical endpoint of a first order phase transition in theories with $m \geq m_0^c$. To test this, we consider a Taylor expansion of $m_c(\mu)$ around $\mu = 0$ and determine the first two coefficients from lattice simulations with staggered fermions on $N_t = 4$ lattices. We employ two different techniques: a) calculating the coefficients directly from a $\mu = 0$ ensemble using a novel finite difference method, and b) fitting them to simulation data obtained for imaginary chemical potentials. The μ^2 and μ^4 coefficients are found to be negative by both methods, with consistent absolute values. Combining both methods gives evidence that also the μ^6 coefficient is negative. Hence, on coarse $N_t = 4$ lattices a three-flavour theory with $m > m_0^c$ does not possess a *chiral* critical endpoint for quark chemical potentials $\mu \lesssim T$. Simulations on finer lattices are required for reliable continuum physics. Possible implications for the QCD phase diagram are discussed.

1 Introduction

The understanding of the QCD phase diagram as a function of temperature and baryon density plays an important role in an increasing number of nuclear and particle physics programmes, with possible applications to cosmology and astro-particle physics. Of particular interest in the context of heavy ion collision experiments is the location and nature of the quark-hadron transition. The generally expected picture – with an analytical crossover at $\mu = 0$ turning into a first order transition beyond some critical chemical potential μ_E – is based on combining lattice results for $\mu = 0$ with model calculations at $\mu \neq 0$ and connecting various limiting cases by universality and continuity arguments [1]. In particular it is generally believed that, in the enlarged parameter space $\{m_{u,d}, m_s, T, \mu\}$, the critical endpoint of QCD with physical quark masses is continuously connected to the chiral critical line at $\mu_E = 0$, which delimits the quark mass region with a first order chiral phase transition at zero density.

The schematic situation at $\mu = 0$ is depicted in Fig. 1 (left). In the limits of zero and infinite quark masses (lower left and upper right corners), order parameters corresponding to the breaking of a global symmetry can be defined, and one numerically finds first-order phase transitions at small and large quark masses at some finite temperatures $T_c(m)$. On the other hand, one observes an analytic crossover at intermediate quark masses, with second order boundary lines separating these regions. Both lines have been shown to belong to the $Z(2)$ universality class of the $3d$ Ising model [3, 4, 5]. The chiral critical line has been mapped out on $N_t = 4$ lattices, and the physical point is confirmed to be on the crossover side of this line [6, 7]. The continuity arguments in [1] suggest that this line should shift with μ towards larger quark masses, thus increasing the region of a chiral first order transition. At some value μ_E it passes through the physical point, whence it represents the endpoint of the phase diagram for physical QCD, Fig. 1 (middle).

This scenario has recently been called into question by numerical simulations at imaginary chemical potential $\mu = i\mu_i, \mu_i \in \mathbb{R}$ [6]. There it was found that, as a function of μ_i, the chiral critical line moves towards larger quark masses. In the degenerate $N_f = 3$ theory and in the neighbourhood of the critical point $m_{u,d}^c = m_s^c \equiv m_0^c$, the dependence of the critical temperature and quark mass on the chemical potential can be described by a Taylor expansion, with only even powers of μ due to CP-symmetry,

$$\frac{T_c(m, \mu)}{T_c(m_0^c, 0)} = 1 + \sum_{k,l=1} \alpha_{kl} \left(\frac{m - m_0^c}{\pi T_c}\right)^k \left(\frac{\mu}{\pi T_c}\right)^{2l}, \tag{1}$$

$$\frac{m_c(\mu)}{m_c(0)} = 1 + \sum_{k=1} c_k \left(\frac{\mu}{\pi T_c}\right)^{2k}. \tag{2}$$
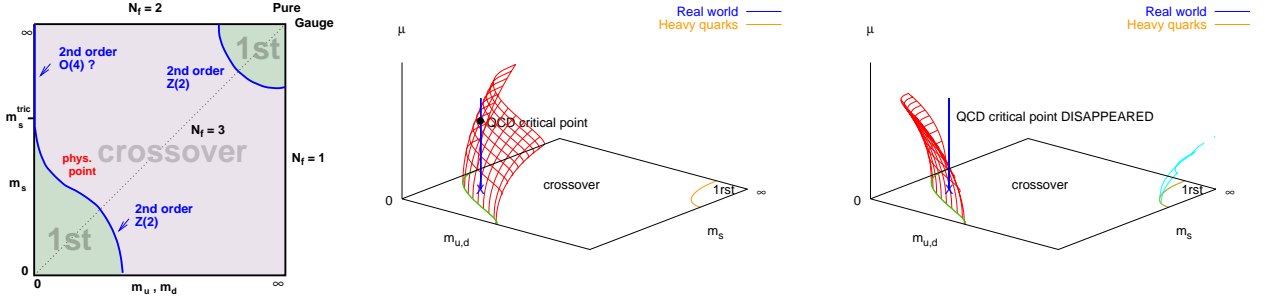
Figure 1: Left: Schematic phase transition behaviour of $N_f = 2 + 1$ QCD for different choices of quark masses $(m_{u,d}, m_s)$ at $\mu = 0$. Middle/Right: Critical surface swept by the chiral critical line as μ is turned on. Depending on the curvature, a QCD chiral critical point is present or absent [2]. For heavy quarks the curvature has been determined [5] and the first order region shrinks with μ.

By performing simulations at several values of μ_i and quark masses, the leading coefficients were determined, and in particular c_1 was found to be negative. This implies a scenario as in Fig. 1 (right), where the chiral critical line does not cross the physical point for small (real) chemical potentials. If this behaviour continues to larger values of μ, there would be no non-analytic chiral phase transition or end point at all in physical QCD.

Clearly, it is now important to assess the reliability of this result. The main systematic uncertainties associated with the calculation in [6] are the truncation of the Taylor expansion Eq. (2) and the coarse lattice with $N_t = 4, a \sim 0.3$ fm. In this letter we perform a systematic investigation of the former. Firstly, instead of extracting the leading term in Eq. (2) from fits to a truncated Taylor series, we instead calculate the derivative with respect to μ^2 directly. Our calculation confirms the negative sign of the leading term on two different volumes and with drastically reduced errors. Second, we repeat our fits to Taylor series with vastly increased statistics and simulations at additional values of chemical potentials. This allows us to also constrain the $\mathcal{O}(\mu^4)$ and the sign of the $\mathcal{O}(\mu^6)$ terms, which we both find to be negative as well. Moreover, our leading and next-to-leading order coefficients agree within statistical errors between the two methods. Our findings leave little doubt that on coarse $N_t = 4$ lattices with staggered fermions the scenario Fig. 1 (right) is realised.

2 Extracting the μ dependence of the critical point

Our strategy to determine the μ dependence of the critical quark masses has been described in detail in [6]. In order to keep this paper self-contained, we repeat the essential formulae. On the lattice, the critical parameters Eqs. (1,2) get replaced by critical couplings, which in turn have a Taylor expansion around the zero density critical quark mass,

$$\beta_c(am, a\mu) \;=\; \beta_c(am_0^c, 0) + \sum_{k,l=1} c_{kl} \,(am - am_0^c)^k \,(a\mu)^{2l}, \tag{3}$$

$$am^c(a\mu) \;=\; am_0^c + \sum_{k=1} c_k' \,(a\mu)^{2k} \;. \tag{4}$$

As in our previous investigations, our observable for criticality is the Binder cumulant constructed from the fluctuations of the chiral condensate,

$$B_4 \equiv \frac{\langle (\delta\bar{\psi}\psi)^4 \rangle}{\langle (\delta\bar{\psi}\psi)^2 \rangle^2}, \quad \delta\bar{\psi}\psi = \bar{\psi}\psi - \langle \bar{\psi}\psi \rangle. \tag{5}$$

In the infinite volume limit the Binder cumulant behaves discontinuously, assuming the values 1 in a first order regime, 3 in a crossover regime and 1.604 characteristic of the $3d$ Ising universality at a second order chiral critical point. In a finite volume the discontinuities are smeared out and flattened, so that B_4 passes continuously through the critical value, i.e. it is an analytic function of $(\beta, am, a\mu)$. For a given pair $(am, a\mu)$, the gauge coupling needs to be fixed to its pseudo-critical value $\beta_c(am, a\mu)$ by requiring, for instance, that the susceptibility $\langle (\delta X)^2 \rangle$ be maximum. We use the equivalent prescription of requiring a vanishing third moment, $M_3 \equiv \langle (\delta X)^3 \rangle = 0$. In the neighbourhood of the chiral critical point the Binder cumulant can then be expanded as

$$B_4(am, a\mu) = 1.604 + \sum_{k,l=1} b_{kl} \,(am - am_0^c)^k (a\mu)^{2l} \;, \tag{6}$$

with volume dependent coefficients $b_{kl}(L)$.

For large volumes the approach to the thermodynamic limit is governed by universality. Near a critical point the correlation length diverges as $\xi \sim r^{-\nu}$, where r is the distance to the critical point in the plane of temperature and magnetic field-like variables, and $\nu \approx 0.63$ for the $3d$ Ising universality class. Since β is tuned to β_c always, we have $r \propto |am - am_0^c|$ for $\mu = 0$ and $r \propto |a\mu|^2$ for $am = am_0^c$. B_4 is a function of the dimensionless ratio L/ξ, or equivalently $(L/\xi)^{1/\nu}$. Hence, for the Taylor coefficients one expects, for large volumes, the universal scaling behaviour

$$b_{kl}(L) = f_{kl} L^{(k+l)/\nu} \;, \tag{7}$$

3

where the f_{kl} are independent of the volume.

It is now straightforward to relate the desired coefficients in Eq. (4) to those appearing in the Binder cumulant Eq. (6). The function $am^c(a\mu)$ is defined implicitly by the condition that the Binder cumulant stays critical, $B_4(am, a\mu) = 1.604$. Taking total derivatives with respect to μ^2 one obtains

$$
\begin{aligned}
c_1' &= \frac{d\,am^c}{d(a\mu)^2} = -\frac{\partial B_4}{\partial(a\mu)^2}\left(\frac{\partial B_4}{\partial am}\right)^{-1} = -\frac{b_{01}}{b_{10}} \quad, \\
c_2' &= \frac{1}{2!}\frac{d^2\,am^c}{d[(a\mu)^2]^2} = -\frac{1}{b_{10}}(b_{02} + b_{11}c_1' + b_{20}c_1'^2) \quad, \\
c_3' &= \frac{1}{3!}\frac{d^3\,am^c}{d[(a\mu)^2]^3} = -\frac{1}{b_{10}}(b_{03} + b_{11}c_2' + b_{12}c_1' + b_{21}c_1'^2 + 2b_{20}c_1'c_2' + b_{30}c_1'^3) \quad. \quad (8)
\end{aligned}
$$

Once these coefficients are known, they need to be converted to the continuum coefficients Eq. (2). This is non-trivial: for fixed temporal lattice extent N_t the lattice spacings entering the dimensionless $am^c(\mu)$ and $am^c(0)$ are different, since the pseudo-critical temperature $T_c(m_c(\mu), \mu) = 1/(N_t a(\mu))$ depends on μ. The relation between the continuum and lattice coefficients is thus

$$
\begin{aligned}
c_1 &= \frac{\pi^2}{N_t^2}\frac{c_1'}{am_0^c} + \frac{1}{T_c(m_0^c, 0)}\frac{dT_c(m^c(\mu), \mu)}{d(\mu/\pi T)^2}, \\
c_2 &= \frac{\pi^4}{N_t^4}\frac{c_2'}{am_0^c} - \frac{\pi^2}{N_t^2}\frac{c_1'}{am_0^c}\frac{1}{T_c(m_0^c, 0)}\frac{dT_c(m^c(\mu), \mu)}{d(\mu/\pi T)^2} \\
&\quad + \frac{1}{2T_c(m_0^c, 0)}\frac{d^2 T_c(m^c(\mu), \mu)}{d[(\mu/\pi T)^2]^2} \quad.
\end{aligned} \quad (9)
$$

The pseudo-critical temperature $T_c(m, \mu)$ can be obtained from $\beta_c(am, a\mu)$ by means of the two-loop beta-function. Note that for our coarse lattices $N_t = 4$ this procedure is certainly not quantitatively valid, and some non-perturbative beta-function should be used. However, we shall see that for the conclusions to be drawn later the two-loop beta-function is actually sufficient.

With these equations, we are ready for numerical evaluations. Our task is to extract the coefficients b_{kl} of the Binder cumulant expansion, Eq. (6), from numerical simulations, and then convert them to the continuum via Eqs. (8,9). In the following sections we present results for two independent ways of measuring the b_{kl}.

3 Calculating derivatives

When attempting to extract Taylor coefficients by fits of truncated series to data containing the full μ-dependence at imaginary μ, one has to worry about systematic errors.

Fitting to a finite polynomial necessarily distributes the actual μ-dependence across the available terms, and the result is only reliable to the extent that the higher terms are numerically negligible. In particular, leading order fits run a risk of "averaging" a more complicated functional dependence into a single coefficient, especially when the function is very flat. These dangers have recently been demonstrated for the pseudo-critical coupling in SU(2), where calculations at real μ are possible and can be compared to results obtained via analytic continuation from imaginary μ [8].

To guard against this, and because the μ-dependence of B_4 is extremely weak [6], we now wish to calculate the derivative $\partial B_4/\partial(a\mu)^2$ directly, without recourse to fitting. (For $\partial B_4/\partial(am)$ this is not necessary, the m-dependence of B_4 is pronounced enough to give reliable fits [4, 6]). In principle, this can be done by expressing the $\mu-$derivative of B_4 analytically through traces of non-local operators, whose expectation values are to be evaluated at $\mu = 0$. This technique has been used to calculate the Taylor coefficients of the pseudo-critical temperature, the pressure and various susceptibilities in [9, 10]. However, we do not follow this approach here. First, the numerical effort is non-trivial. For instance, the trace of the 5th inverse power of the Dirac operator must be evaluated to obtain the derivative of $(\delta\bar{\psi}\psi)^4$ with respect to the quark mass. Moreover, delicate cancellations will take place among the rapidly growing number of terms, leading to difficulties with optimising the number of noise vectors to be used as accurate stochastic estimators of the various traces.

Instead, we use a new method to estimate the derivative, which turns out to be simpler to implement and vastly more efficient. We measure the change ΔB_4 under a small variation $\Delta(a\mu)^2$, thus estimating the ratio of finite differences which, for sufficiently small variations, approaches the desired derivative,

$$\lim_{\Delta(a\mu^2)\to 0} \frac{\Delta B_4}{\Delta(a\mu)^2} = \left.\frac{\partial B_4}{\partial(a\mu)^2}\right|_{\mu=0}. \tag{10}$$

Because the required shift in the couplings is very small, it is adequate and safe to use the original Monte Carlo ensemble for $am_0^c, \mu = 0$ and reweight the results by the standard Ferrenberg-Swendsen method [11]. Moreover, reweighting to imaginary μ the reweighting factors remain real positive and close to 1. With reweighting, the fluctuations in the original and the reweighted ensembles are strongly correlated. For the calculation of variations this is beneficial. The correlated fluctuations drop out of our observable, which now is the *change* in B_4, rather than B_4 itself. As a final simplification, we do not calculate the reweighting factors

$$\rho(\mu_1, \mu_2) = \frac{\det^{N_f/4} \not{D}(U, \mu_2)}{\det^{N_f/4} \not{D}(U, \mu_1)} \tag{11}$$
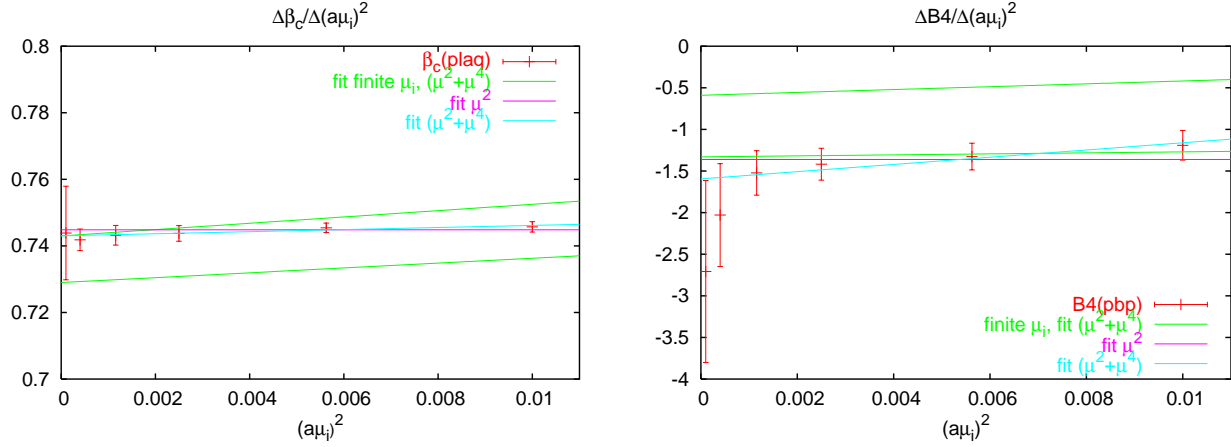
5

Figure 2: Finite difference quotients on $L = 8$ extrapolated to zero as a constant, or constant plus $(a\mu_i)^2$ correction. The resulting coefficients are listed in Table 1. The error band corresponds to the highlighted best fits to data at imaginary μ, Table 2.

exactly, but estimate them through Gaussian noise vectors η in the standard way,

$$\rho(\mu_1, \mu_2) = \left\langle \exp\left(-|\slashed{D}^{-N_f/8}(\mu_2)\slashed{D}^{+N_f/8}(\mu_1)\eta|^2 + |\eta|^2\right)\right\rangle_\eta. \qquad (12)$$

As a further check of the method on a more accurately calculable observable, we also consider the pseudo-critical coupling β_c defined by the peak of the plaquette susceptibility, and calculate $\partial\beta_c/\partial(a\mu)^2$ along the way. Further details and a thorough test of this method in the Potts model are described in [12], where the results were found to fully agree with the other method of computing derivatives. Since that test the technique has also been successfully applied in a similar calculation at finite isospin chemical potential [13].

Our calculations for $\partial\beta_c/\partial(a\mu)^2$, $\partial B_4/\partial(a\mu)^2$ were done on $8^3 \times 4$ and $12^3 \times 4$ lattices, for which we have accumulated about 5 million and 0.5 million trajectories, respectively [1]. The bare quark mass was kept fixed at $am = 0.0265$, which is close to the critical value am_0^c and corresponds to $m_\pi L \sim 3.4, 5$, respectively. (A small offset from am_0^c will affect the μ-derivative only via the lowest order mixing term, whose coefficient is compatible with zero, as we shall see in the next section.) The results of this calculation are shown in Fig. 2. The individual data points correspond to the difference quotient reweighted to the given value of μ_i. The error bars within one plot are thus strongly correlated. The straight lines represent linear extrapolations to zero μ_i, and

---

[1]The $8^3 \times 4$ simulations were performed in about two months on the EGEE computing grid, thanks to the support of the CERN IT/GS group. Jobs at different parameter sets were distributed on the grid infrastructure where typically ~ 1000 CPUs could be used at the same time for this activity.

c_{01}	c_{02}	χ^2/dof	b_{01}	b_{02}	f_{01}	f_{02}	χ^2/dof
0.7448(6)	—	0.38	1.36(8)	—	0.050(3)	—	0.82
0.7430(6)	0.31(9)	0.12	1.59(12)	43.4(18.8)	0.059(4)	0.059(26)	0.33
0.737(3)	—	1.10	2.63(40)	—	0.051(8)	—	0.50
0.7430(6)	0.14(1.10)	1.37	3.35(53)	259.0(148.0)	0.065(10)	0.097(56)	0.44

Table 1: Taylor coefficients of $\beta_c(am, a\mu)$ and $B_4(am, a\mu)$, Eqs. (3,6,7), from the extrapolated finite differences, as shown in Fig. 2. The upper rows are for $L = 8$, the lower rows for $L = 12$.

the intercept is the final estimate for the respective derivatives. The extrapolations with non-zero slope show the influence of the next-to-leading term. All estimates are collected in Table 1.

Next, we can check for finite volume scaling between our two volumes. This is done in Fig. 3, where the difference quotients are plotted against a volume-rescaled variable. The pseudo-critical coupling has a finite thermodynamic limit, so its Taylor coefficients should become volume-independent once the lattices are large enough. On the other hand, B_4 has to scale in a way characteristic of the $3d$ Ising universality according to Eq. (7). The rescaled curves in Fig. 3 nearly fall on top of each other, i.e. both large volume scaling behaviours are realised to a good approximation between our $L = 8$ and $L = 12$ lattices.

4   Simulations at imaginary μ

In this section we revisit our earlier attempt [6] to determine the Taylor coefficients from simulations at non-vanishing imaginary $\mu = i\mu_i$, for which there is no sign problem. In this case the data contain no approximation other than the discretisation, and can be fitted by the truncated series Eqs. (3,6) directly. As in [6], we consider an $8^3 \times 4$ lattice, but we have added some more values of μ_i and increased the statistics. We measured B_4 for 42 different pairs $(am, a\mu)$ drawn from $am \in [0.020, 0.034], \mu_i \in [0, 0.262]$, each pair simulated at 3-5 different β-values around the pseudo-critical one. Our overall statistics is well over 20 million trajectories.

Fits of Eqs. (3,6) to various orders are collected in Table 2. The first column specifies the fitting range, i.e. the maximal imaginary chemical potential included in the fits. We observe that β_c can be fitted across the entire range, whereas for B_4 excellent fits are obtained up to $a\mu_i = 0.245$. Once the fitting range is further increased, the χ^2
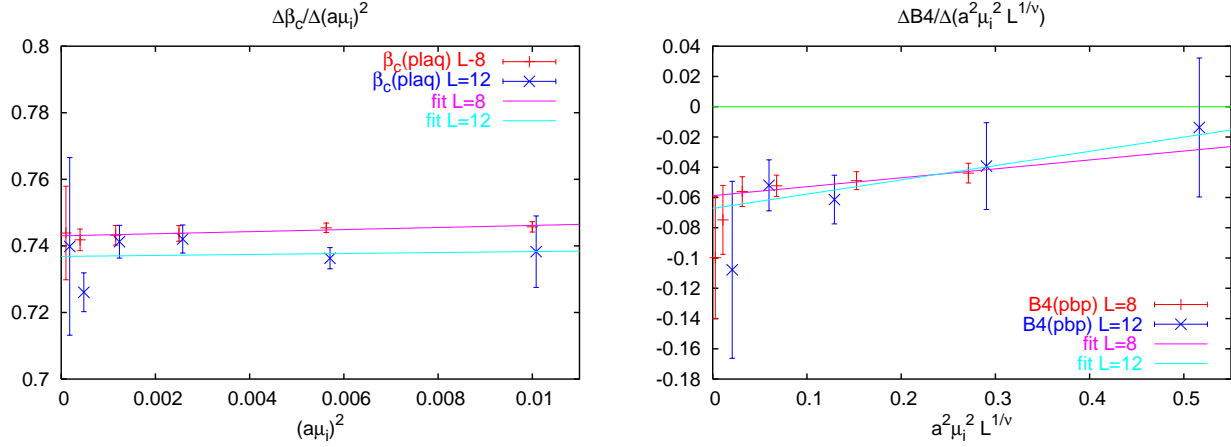
Figure 3: Finite size scaling of the Taylor coefficients between $L = 8, 12$ lattices. For the pseudo-critical coupling, finite size corrections disappear in the thermodynamic limit. B_4 is expected to scale according to Eq. (7).

abruptly grows, and the values for the coefficients change. Clearly, this indicates the need for higher order terms. Furthermore, for large μ_i there is a phase transition to an unphysical Z(3)-sector [14], which for $N_t = 4$ happens at $a\mu_i = \frac{\pi}{3N_t} \approx 0.262$. Hence, close to this point the scaling behaviour of this Z(3) transition will mix into B_4, masking that of the transition we are after and leading to large finite volume effects. For these reasons we discard fitting ranges $a\mu_i > 0.245$. This does not affect β_c, because it has a finite thermodynamic limit across the entire range.

For the good fits with $\chi^2/\text{dof} < 1.5$, all coefficients are stable within errors under variations of the fitting range. Interestingly, we have a rather solid signal for a vanishing of the lowest order mixing between the m- and μ-dependence in both observables. We quote the highlighted fits as our results for the Taylor coefficients from fits to imaginary μ data.

The estimates for the leading terms agree within errors, while the subleading terms show some differences. The tendency for both coefficients is towards a smaller absolute value than that found by the derivative method. The extended fitting ranges already suggest that this is due to the neglect of higher order terms. Nevertheless, within one and a half standard deviations, also the sub-leading terms are consistent with those from the direct calculation of the derivatives, as is also visible in Fig. 2. We conclude that both methods considered here are able to provide the leading coefficient of the Taylor series in μ quantitatively, as well as at least the sign of the sub-leading coefficients, though the derivative method is much more economical.

8

$|\mu|_{max}$	$\beta(am_0^c, 0)$	c_{10}	c_{20}	c_{01}	c_{02}	c_{11}	χ^2/dof
0.2	5.1354(1)	1.95(3)	-14.1(2.7)	-0.75(1)	0.40(35)	-0.8(1.2)	0.53
0.2	5.1353(1)	1.97(2)	-13.5(2.5)	-0.75(1)	0.43(35)	—	0.52
0.2	5.1352(1)	1.90(2)	—	-0.763(6)	—	—	1.14
0.245	5.1354(1)	1.96(3)	-14.4(2.1)	-0.735(7)	0.84(12)	-0.31(78)	0.52
0.245	5.1354(1)	1.97(2)	-14.5(2.1)	-0.736(7)	0.84(11)	—	0.51
0.245	5.1348(2)	1.89(2)	—	-0.783(5)	—	—	2.17
0.262	5.1354(1)	1.96(3)	-15.2(2.3)	-0.729(8)	1.00(11)	-0.61(86)	0.64
0.262	5.1354(1)	1.98(2)	-15.4(2.3)	-0.729(7)	0.99(11)	—	0.63
$|\mu|_{max}$	am^c	b_{10}	b_{20}	b_{01}	b_{02}	b_{11}	χ^2/dof
0.1	0.0259(4)	14.0(7)	—	0.70(21)	—	—	1.32
0.2	0.0257(4)	14.0(1.5)	-404.8(119)	0.38(58)	-7.2(14.2)	-63.4(54)	0.97
0.2	0.0259(4)	14.0(7)	—	0.70(21)	—	—	1.32
0.235	0.0257(4)	14.7(1.3)	-256.5(99)	0.97(40)	11.7(6.3)	-6.9(28)	1.08
0.235	0.0257(4)	14.9(6)	-256.4(97)	0.98(39)	11.9(6.1)	—	1.05
0.245	0.0257(4)	14.6(1.3)	-255.7(93)	0.96(38)	11.4(5.7)	-8.1(27)	1.00
0.245	0.0257(4)	14.9(6)	-254.9(92)	0.96(37)	11.6(5.6)	—	0.97
0.255	0.0255(4)	15.6(1.5)	-321.1(118)	1.46(46)	22.2(6.8)	9.4(34)	1.59
0.255	0.0255(4)	15.3(8)	-322.4(116)	1.47(46)	22.1(6.6)	—	1.59
0.262	0.0254(5)	16.5(1.6)	-311.4(126)	1.96(47)	32.2(6.7)	-33.1(35)	1.98
0.262	0.0252(5)	15.3(9)	-308.8(126)	2.02(48)	32.4(6.7)	—	1.98

Table 2: Fits of the Taylor expansions $\beta_c(am, a\mu)$, Eq. (3), (upper section) and $B_4(am, a\mu)$, Eq. (6), (lower section) to data at imaginary μ. The first column specifies the fitting range.

5   Comparing and combining approaches

We now have obtained compatible results from two independent methods of calculating the leading Taylor coefficients of power series of critical parameters in $a\mu$. We stress again that these are not merely two ways of analysing the same data. Rather, the simulations required for the two approaches also differ. Furthermore, the derivative method Sec. 3 uses small chemical potentials $|a\mu_i| \leq 0.1$, whereas the finite-μ_i simulations Sec. 4 consider larger values $|a\mu_i| \geq 0.1$. The two approaches are thus

b_{10}	b_{20}	b_{02}	b_{03}	b_{21}	χ^2/dof
14.8(6)	-421.7(177)	49.4(8.3)	469.6(150)	-4950.5(4142)	1.05
14.9(6)	-243.8(96)	47.4(8.2)	421.9(145)	—	1.06
15.0(7)	-208.3(184)	23.5(1.4)	—	-1470.7(4495)	1.33
15.0(7)	-156.8(101)	23.7(1.3)	—	—	1.31

Table 3: Fits of $B_4(am, a\mu)$, Eq. (6), to imaginary μ data, with the leading coefficients $am_0^c = 0.0259, b_{01} = 1.6$ fixed to their values determined at $\mu = 0$.

complementary, and it is reasonable to combine their results in order to maximise the available information. To start with, the critical quark mass at zero density, am_0^c, and b_{01} are best determined from the $\mu = 0$ calculations of Sec 3. Then, these values can be used as input for the fits to a set of imaginary μ data. This is shown in Table 3, where we have fixed $am_0^c = 0.0259$ and $b_{01} = 1.6$, according to our best estimates from $\mu = 0$ simulations.

With two coefficients fixed, we can actually consider the next order in B_4, i.e. add terms $\mathcal{O}(m^3, m^2\mu^2, m\mu^4, \mu^6)$, and still get sensible fits. We find $b_{30} = b_{21} = 0$ in all combinations of fit parameters. Removing the entirely unconstrained coefficients one by one, we observe that b_{03} is the most significant coefficient at this order. Note also that allowing for b_{03}, the value of b_{02} relaxes precisely to the value obtained from the derivative method, Table 1. The same phenomenon is observed for the μ^2 coefficient when releasing μ^4. Since b_{01}, b_{02}, b_{03} all have the same sign, this is not surprising. At imaginary $\mu = i\mu_i$ consecutive terms alternate in sign, and thus show a tendency to cancel each other out. This demonstrates the "averaging" into lower order coefficients of higher order terms that get significant but are excluded from a fit. For these reasons we believe the highlighted fit in Table 3, with b_{03} released, to be the most trustworthy one. Consistency between the two methods is also illustrated in Fig. 4, where we show the data for the reweighted finite difference quotients together with those determined from the direct measurements of B_4 at finite $\mu = i\mu_i$.

We conclude that by combining both methods discussed here, we are sensitive to the μ^6-term. Its main effect is to give us some confidence in the order of magnitude of the μ^4 term determined in our earlier analyses. Moreover, without taking the value of b_{03} too seriously, it comes with the same sign as b_{01} (see Fig. 4), thus leading to a negative c_3'. Hence, the μ^6-term also contributes to the shrinking of the first order region.
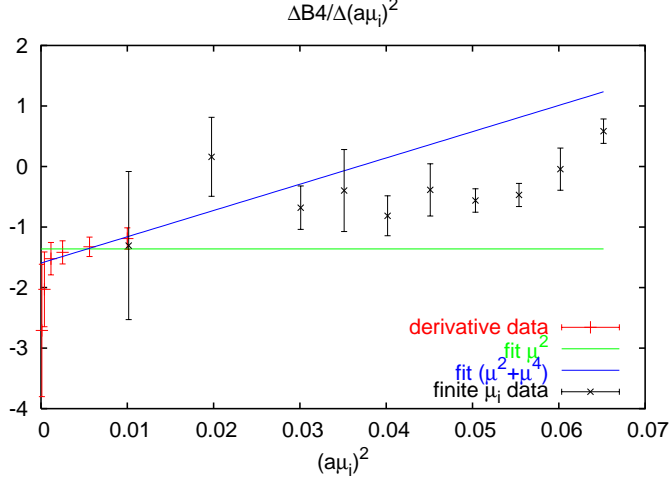
Figure 4: Finite difference quotients on $L = 8$ lattices for $am = 0.0265$. The left section $(a\mu_i)^2 \leq 0.01$ is determined via reweighting, the right section $(a\mu_i)^2 \geq 0.01$ via direct measurements of B_4 at finite $\mu = i\mu_i$. The points at larger values clearly fall below the $\mathcal{O}(\mu^4)$ contribution, thus indicating a negative μ^6-term.

6   Conclusions

For the continuum conversion, Eq. (9), we need the change of temperature at the critical point with μ. This is most conveniently extracted by evaluating the pseudo-critical couplings at the critical points, fitting as a series in $(a\mu)^2$ and converting to temperatures by the two-loop beta-function. Putting it all together, our final result reads[2]

$$\frac{m_c(\mu)}{m_c(0)} = 1 - 3.3(3) \left(\frac{\mu}{\pi T_c}\right)^2 - 47(20) \left(\frac{\mu}{\pi T_c}\right)^4 - \dots \tag{13}$$

We conclude that our investigation of higher order contributions in μ^2 fully supports and sharpens the conclusions of [6]: the light mass range featuring a first order phase transition is shrinking with chemical potential. The quoted errors include one standard deviation uncertainty on the coefficients of the critical temperature, as well as on the parameters m_0^c, b_{01} calculated at $\mu = 0$. They do not include, however, the systematic error introduced by using the two-loop beta-function.

Nevertheless, our conclusion is stable against the use of another beta-function, as can be seen from Eq. (9). The contribution of the second term to c_1 is always negative,

---

[2]We note that the preliminary result $c_2 = -12(6)$ reported earlier at various conferences [15] corresponds to the value obtained from fits to imaginary μ data alone.

irrespective of the beta-function used. For c_2, the first term is numerically dominant and the second is guaranteed to be negative too, no matter what the beta-function. The third term presently also gives a negative contribution, and it is hard to see how a change in beta-function would change the sign and overhaul the contribution of the first two terms. Finally, we have good evidence that c_3' is also negative, i.e. the μ^6 term further shrinks the first order region, at least in lattice units.[3] Thus, all terms appear to have negative signs, confirming our conclusion irrespective of their precise quantitative values.

Our result therefore demonstrates beyond reasonable doubt that for $N_f = 3$ the region of first order chiral phase transitions *shrinks* for small to moderate μ/T, as in Fig. 1 (right), and hence there is *no* chiral critical point at chemical potentials $\mu \lesssim T$ in a theory with three flavours of staggered fermions and $m > m_0^c$ on an $N_t = 4$ lattice. In order to draw conclusions for physical QCD, two further steps are necessary. Firstly, the investigation has to be generalised to $N_f = 2 + 1$. Secondly, and most importantly, it has to be repeated on finer lattices, since $N_t = 4$ with $a \sim 0.3$ fm is too coarse to accurately reflect continuum physics. It is by no means excluded that cut-off effects are stronger than finite density effects on coarse lattices, and hence a change of sign in the curvature of the chiral critical surface in the continuum is a possibility. Simulations to address these issues are in progress. Finally, we emphasise that our findings only concern a *chiral* critical point, i.e. a point on the critical surface in Fig. 1 bounding the region of first-order chiral transitions. Our results do not exclude an additional critical surface in Fig. 1 (right), not analytically connected to the region of chiral phase transitions, which could cause a critical point and phase transition of a different nature to exist.

Acknowledgements:

---

[3]We have not converted this coefficient to the continuum because we cannot quantify all terms in Eq. (9) with sufficient accuracy at present.

References

[1] A. M. Halasz *et al.*, Phys. Rev. D **58** (1998) 096007 [arXiv:hep-ph/9804290]; M. A. Stephanov, K. Rajagopal and E. V. Shuryak, Phys. Rev. Lett. **81** (1998) 4816 [arXiv:hep-ph/9806219]; K. Rajagopal and F. Wilczek, arXiv:hep-ph/0011333;

[2] O. Philipsen, Eur. Phys. J. ST **152** (2007) 29 [arXiv:0708.1293 [hep-lat]]; E. Laermann and O. Philipsen, Ann. Rev. Nucl. Part. Sci. **53** (2003) 163 [arXiv:hep-ph/0303042].

[3] F. Karsch, E. Laermann and C. Schmidt, Phys. Lett. B **520** (2001) 41 [arXiv:hep-lat/0107020].

[4] P. de Forcrand and O. Philipsen, Nucl. Phys. B **673** (2003) 170 [arXiv:hep-lat/0307020].

[5] S. Kim, Ph. de Forcrand, S. Kratochvila and T. Takaishi, PoS **LAT2005**, (2006) 166 [arXiv:hep-lat/0510069].

[6] P. de Forcrand and O. Philipsen, JHEP **0701** (2007) 077 [hep-lat/0607017].

[7] Y. Aoki *et al.*, Nature **443** (2006) 675 [hep-lat/0611014].

[8] P. Cea, L. Cosmai, M. D'Elia and A. Papa, Phys. Rev. D **77** (2008) 051501 [arXiv:0712.3755 [hep-lat]].

[9] C. R. Allton *et al.*, Phys. Rev. D **66** (2002) 074507 [arXiv:hep-lat/0204010].

[10] R. V. Gavai and S. Gupta, Phys. Rev. D **71** (2005) 114014 [arXiv:hep-lat/0412035].

[11] A. M. Ferrenberg and R. H. Swendsen, Phys. Rev. Lett. **63** (1989) 1195.

[12] P. de Forcrand, S. Kim and O. Philipsen, PoS **LAT2007** (2007) 178 [arXiv:0711.0262 [hep-lat]].

[13] J. B. Kogut and D. K. Sinclair, Phys. Rev. D **77** (2008) 114503 [arXiv:0712.2625 [hep-lat]].

[14] A. Roberge and N. Weiss, Nucl. Phys. B **275** (1986) 734.

[15] Ph. de Forcrand, arXiv:0807.0860 [hep-lat]; O. Philipsen, arXiv:0808.0672 [hep-ph].